Free Radical Biology & Medicine 50 (2011) 37–46

Contents lists available at ScienceDirect

Free Radical Biology & Medicine

journal homepage: www.elsevier.com/locate/freeradbiomed

Original Contribution

Functional characterization of methionine sulfoxide reductase A from *Trypanosoma* spp.

Diego G. Arias [a], Matías S. Cabeza [a], Esteban D. Erben [b], Pedro G. Carranza [c], Hugo D. Lujan [c], María T. Téllez Iñón [b], Alberto A. Iglesias [a], Sergio A. Guerrero [a,*]

[a] *Instituto de Agrobiotecnología del Litoral, UNL-CONICET, 3000 Santa Fe, Argentina*
[b] *Instituto de Investigaciones en Ingeniería Genética y Biología Molecular (INGEBI-CONICET) and Facultad de Ciencias Exactas y Naturales, Universidad de Buenos Aires, Buenos Aires, Argentina*
[c] *Laboratorio de Bioquímica y Biología Molecular, Facultad de Medicina, Universidad Católica de Córdoba, Córdoba, Argentina*

ARTICLE INFO

Article history:
Received 31 August 2010
Revised 28 September 2010
Accepted 13 October 2010
Available online 20 October 2010

Keywords:
Trypanosoma
Methionine sulfoxide
Trypanothione
Oxidative stress
Tryparedoxin
Free radicals

ABSTRACT

Methionine is an amino acid susceptible to being oxidized to methionine sulfoxide (MetSO). The reduction of MetSO to methionine is catalyzed by methionine sulfoxide reductase (MSR), an enzyme present in almost all organisms. In trypanosomatids, the study of antioxidant systems has been mainly focused on the involvement of trypanothione, a specific redox component in these organisms. However, no information is available concerning their mechanisms for repairing oxidized proteins, which would be relevant for the survival of these pathogens in the various stages of their life cycle. We report the molecular cloning of three genes encoding a putative A-type MSR in trypanosomatids. The genes were expressed in *Escherichia coli,* and the corresponding recombinant proteins were purified and functionally characterized. The enzymes were specific for L-Met(*S*)SO reduction, using *Trypanosoma cruzi* tryparedoxin I as the reducing substrate. Each enzyme migrated in electrophoresis with a particular profile reflecting the differences they exhibit in superficial charge. The in vivo presence of the enzymes was evidenced by immunological detection in replicative stages of *T. cruzi* and *Trypanosoma brucei*. The results support the occurrence of a metabolic pathway in *Trypanosoma* spp. involved in the critical function of repairing oxidized macromolecules.

All aerobic organisms are exposed to reactive oxygen species (ROS) generated during cellular respiration and able to react with numerous macromolecules [1]. There is evidence about the relationships between oxidative stress and cellular damage, aging, and several pathological situations such as arthritis and Alzheimer, cardiovascular, and other neurodegenerative diseases [2]. Hence, several protective systems (catalase, peroxidase, superoxide dismutase, and glutathione-associated enzymes) help the cell to eliminate or minimize these injurious molecular species [1]. Additionally, there are enzymes responsible for DNA or protein rescue after the occurrence of oxidative damage. It is known that protein oxidation can generate conformational changes and, in some cases, loss of function [3]. The amino acids most susceptible to oxidation are cysteine, histidine, tryptophan, tyrosine, and methionine [3]. Oxidation of methionine to methionine sulfoxide (MetSO) produces a mixture of epimers on the sulfur atom [Met(*S*)SO and Met(*R*)SO] [4], affecting the biological function of the oxidized protein [3]. Consequently, the occurrence of a system for reducing MetSO to Met does matter in the cell. Such a reaction is catalyzed by the enzyme methionine sulfoxide reductase (MSR), which is present in almost all organisms [2,4]. The enzyme protects the organism from oxidative damage, being essentially involved in resistance against abiotic and biotic stress in plants and animals [5,6]. It can also act as a virulence factor in some bacterial pathogens such as *Neisseria gonorrhoeae* [7], *Staphylococcus aureus* [8], and *Mycobacterium tuberculosis* [9].

Despite the relevance of MSR to the biochemistry and cellular physiology of various organisms, the enzyme has never been characterized in protozoa, especially in those of medical and veterinary importance. At present, two unrelated classes of MSR have been described in several organisms: MSRA, which is stereospecific to the *S* isomer of the sulfur atom in the sulfoxide group [4,10], and MSRB, which is specific to the *R* isomer [4,8]. Several crystalline structures of MSRA and MSRB from various sources have been solved [4]. Both MSRA and MSRB present similar three-step catalytic mechanisms [4]. During the first (reductive) step a sulfenic group is formed on the catalytic cysteine of the enzyme with a concomitant regeneration of Met. Afterward, a second cysteine (resolutive cysteine) attacks the intermediary sulfenic group generating an intrachain disulfide bridge, with elimination of a water molecule.

Abbreviations: GSH, reduced glutathione; L-MetSO, L-methionine sulfoxide; MSR, methionine sulfoxide reductase; TR, trypanothione reductase; TXNI, tryparedoxin I; $T(SH)_2$, reduced trypanothione.

* Corresponding author. Fax: +54 342 457 5221.
E-mail address: sguerrer@fbcb.unl.edu.ar (S.A. Guerrero).

0891-5849/$ – see front matter © 2010 Elsevier Inc. All rights reserved.
doi:10.1016/j.freeradbiomed.2010.10.695

Finally, the enzyme is reduced, preferentially by thioredoxin (TRX), in the last stage of the catalytic cycle.

Trypanosomatids are unicellular organisms of the order Kinetoplastida that parasitize a wide variety of invertebrate and vertebrate hosts. [11]. The most relevant specimens for human and animal health belong to two genera, *Trypanosoma* and *Leishmania,* which produce around half a million human deaths annually worldwide. In sub-Saharan countries, *T. brucei rhodesiense* and *T. brucei gambiense* are the causative agents of African sleeping sickness, and Nagana cattle disease is caused by *T. brucei brucei* [11]. In Latin America, *T. cruzi* is responsible for Chagas disease [11]. Trypanosomatids represent one of the earliest branches of the eukaryotic evolution [12]. The parasites show biochemical peculiarities among living organisms, such as a unique thiol redox metabolism [12]. Genome sequencing projects of *T. brucei* and *T. cruzi* revealed that trypanosomatids lack genes coding for glutathione reductase, TRX reductase, catalase, and selenocysteine-containing glutathione peroxidases [13].

Although in most eukaryotic organisms the glutathione (GSH) and TRX systems are the major components responsible for maintaining the intracellular thiol redox homeostasis, in trypanosomatids redox metabolism mainly is based on a low-molecular-mass dithiol, trypanothione [N_1,N_8-bis(glutathionyl) spermidine; $T(SH)_2$] [12]. For this, trypanothione reductase (TR) catalyzes the NADPH-dependent reduction of oxidized trypanothione (TS_2) to the reduced form $T(SH)_2$, which drives peroxide detoxification through two proteins working together: tryparedoxin (TXN) and a peroxiredoxin (PRX). The trypanothione-dependent system protects the parasite against oxidative damage, as well as poisoning by heavy metals, and also provides reduction equivalents for deoxyribonucleotide synthesis [11]. $T(SH)_2$ is the specific reductant of TXN, a multipurpose redox protein belonging to the TRX superfamily [14]. TXN is a specific reducing substrate for diverse PRXs found in the parasite, including two typical Cys–PRXs and a glutathione peroxidase-like protein [15].

Characterization of the redox metabolism in trypanosomatids is far from being completed [16]. Most of the work carried out in this area emphasizes the analysis of ROS detoxification; but the maintenance of the cellular homeostasis is based not only on detoxification pathways but also on the repair of the oxidative damage of nucleic acids, lipids, and proteins. In this work we describe an enzymatic system involved in the repair of oxidized proteins in *T. cruzi* and *T. brucei.* Our results improve the knowledge and understanding of redox metabolism in parasites of the genus *Trypanosoma* and add value to the genome project database, identifying the occurrence of functional proteins involved in key metabolic routes.

Materials and methods

Materials

Bacteriological medium components were from Britania Laboratories. *Taq* DNA polymerase and the restriction enzymes were from Promega. Trypanothione disulfide was acquired from Bachem. All other reagents and chemicals were of the highest quality commercially available from Sigma. The L-Met(*S*)SO and L-Met(*R*)SO enantiomers were prepared according to Holland et al. [51].

Protozoa and culture procedure

For this study *T. cruzi* CL-Brener cells were used. Epimastigote cells were cultivated axenically at 28 °C in LIT medium supplemented with 10% (w/v) bovine fetal serum and 20 μg ml^{-1} hemin, as was previously reported [17]. Metacyclic trypomastigotes were obtained from axenic cultures under differentiating conditions [18]. Amastigote cells were developed in Vero cell cultures, as previously [19].

Bacteria and plasmids

Escherichia coli Top 10 F′ and *E. coli* BL21(DE3) cells (Invitrogen) were utilized in routine plasmid construction and expression assays. The vector pGEM-T Easy (Promega) was selected for cloning and sequencing purposes. The expression vector was pRSET-A (Invitrogen). DNA manipulation, *E. coli* culture, and transformation were performed according to standard protocols [20].

Molecular cloning of tcrmsr10, tcrmsr180, and tbrmsr genes

Genomic DNAs of the parasites were obtained from epimastigote cells grown at the logarithmic phase as previously described [20]. Genes from *T. cruzi* (*tcrmsr10* and *tcrmsr180*) and *T. brucei* (*tbrmsr*) were amplified from their respective genomic DNA by PCR, using the following oligonucleotide primer pairs designed from known spliced sequences (Pathogen Sequencing Unit, Sanger Institute, Wellcome Trust, http://www.genedb.org/): *Tcr*MSR10 For, *GGATCC*ATGGCTTCTGGTGTTC CAGCG; *Tcr*MSR180 For, *GGATCC*ATGGCTTCTGGTGCTCCAGCG; *Tcr*MSR Rev, *AAGCTT*TTCACCAATGAATTCGGTGCG; *Tbr*MSR For, *GGATCC*AT GAACCCAAATGCTGTTGC; and *Tbr*MSR Rev, *AAGCTT*TCACCAGTAGA GACGGTGTG. Each PCR was performed under the following conditions: 94 °C for 10 min; 30 cycles of 94 °C for 1 min, 60 °C for 1 min, and 72 °C for 1 min; and then 72 °C for 10 min. The PCR product was subsequently purified and ligated into the pGEM-T Easy vector (Promega) to facilitate further work. Fidelity and correctness of each gene were confirmed on both strands by complete sequencing (Macrogen, South Korea).

Construction of the expression vectors

pGEM-T Easy plasmids containing the cloned genes and the pRSET-A vector (Invitrogen) were digested with *Bam*HI and *Hin*dIII. Restriction fragments were purified by gel extraction after gel electrophoresis. Ligation to the pRSET-A vector of each insert was performed using T4 DNA ligase for 16 h at 16 °C. Competent *E. coli* BL21(DE3) cells were transformed with the respective construct. Transformed cells were selected in agar plates containing Luria–Bertani broth (10 g l^{-1} NaCl, 5 g l^{-1} yeast extract, 10 g l^{-1} peptone, pH 7.4) supplemented with ampicillin (100 μg ml^{-1}). Preparation of plasmid DNA and subsequent *Bam*HI/*Hin*dIII digestion were performed to check correctness of the constructs.

Overexpression and purification of recombinant proteins

Single colonies of *E. coli* BL21(DE3) transformed with the respective recombinant plasmid were selected. Overnight cultures were diluted 1/100 in fresh medium (TB broth: 12 g l^{-1} peptone, 24 g l^{-1} yeast extract, 4 ml l^{-1} glycerol, 2.3 g l^{-1} KH_2PO_4, and 12.5 g l^{-1} K_2HPO_4, pH 7.0, supplemented with 100 μg ml^{-1} ampicillin) and grown under identical conditions to exponential phase, OD_{600} 0.6. The expression of the respective recombinant protein was induced with 0.5 mM IPTG, followed by incubation at 25 °C. After 4 h, cells were harvested and stored at −20 °C. Purification of each recombinant protein was performed using a Co^{2+}–IDA–Sepharose resin (GE Healthcare). Briefly, the bacterial pellet was resuspended in binding buffer (20 mM Tris–HCl, pH 8.0, 300 mM NaCl) and disrupted by sonication. The lysate was centrifuged (10,000 *g*, 30 min) to remove cell debris. The resultant crude extract was loaded onto a Co^{2+}–IDA–Sepharose column that had been equilibrated with binding buffer. After being washed with 10 bead volumes of binding buffer plus 10 mM imidazole, the recombinant protein was eluted with elution buffer (20 mM Tris–HCl, pH 8.0, 300 mM NaCl, 500 mM imidazole). Purified enzyme fractions were pooled, concentrated by ultrafiltration, and stored at −80 °C in 20 mM Tris–HCl, pH 7.5, 1 mM EDTA, and 4% (v/v) glycerol. Under the specified storage conditions, the recombinant proteins were stable for at least

12 months. *Tcr*TXNI and *Tcr*TR were obtained according to previous reports [21].

Protein methods

Cell-free extracts were analyzed by SDS–PAGE [22] using the Mini-Protean II (Bio-Rad) apparatus. The final polyacrylamide monomer concentration was 15% (w/v) for the separating gel and 4% (w/v) for the stacking gel. Coomassie brilliant blue was used for protein staining. Protein content was determined by the method of Bradford [23] with bovine serum albumin (BSA) as standard.

Serum anti-*Tcr*MSR10 was prepared by immunization of a rabbit with the purified recombinant proteins according to Vaitukaitis et al. [24]. Parasite protein extracts were prepared by resuspending the parasite pellets in lysis buffer (50 mM Tris–HCl, pH 7.5, 150 mM NaCl, 1% (v/v) Nonidet P-40) with proteinase inhibitors (10 μM L-*trans*-epoxysuccinylleucylamido(4-guanidino) butane, 1 mM phenylmethylsulfonyl fluoride, 25 U ml^{-1} aprotinin, 10 μg ml^{-1} leupeptin) followed by three to five freeze-and-thaw cycles. The complete rupture was confirmed by microscopic visualization. Proteins in SDS–PAGE gels were blotted onto PVDF membranes. The membrane was blocked overnight at 4 °C, subsequently incubated with primary antibody at room temperature for 1 h, and then incubated with a horseradish peroxidase-conjugated anti-rabbit secondary antibody for 1 h. Bands were visualized using the ECL Western blotting detection reagents (PerkinElmer).

Determination of the molecular mass by native PAGE

Determination of molecular mass of proteins was performed by means of native PAGE, 6–10% (w/v), according to Ferguson's method [25]. The calibration curve was constructed using the logarithm of the molecular mass (log MW) vs the square root of the retardation coefficient ($K_D^{0,5}$) measured for each molecular mass standard.

MSR activity assay

MSR activity was measured by monitoring NADPH oxidation at 340 nm by means of a coupled assay that guaranteed the regeneration of *Tcr*TXNI to its reduced form. All enzyme assays were performed at 30 °C, in a final volume of 50 μl, and using a Multiskan Ascent one-channel vertical light-path filter photometer (Thermo Electron Co.). The reaction mixture contained (unless otherwise specified) 100 mM Tris–HCl, pH 7.5, 2 mM EDTA, 300 μM NADPH, 2 U ml^{-1} *Tcr*TR, 100 μM $T(SH)_2$, 10 μM *Tcr*TXNI, and the respective MSR included in a specific range of concentrations (0.5–2 μM *Tcr*MSR10, 0.5–8 μM *Tcr*MSR180, or 0.5–8 μM *Tbr*MSR). Reactions were started by the addition of 2.5 mM L-Met(*S*)SO or L-Met(*R*)SO.

For steady-state kinetic analysis, the assay was performed using 20–2500 μM L-Met(*S*)SO and 0.5–20 μM *Tcr*TXNI. Kinetic data were plotted as initial velocity (μM min^{-1}) versus substrate concentration (μM). The kinetic constants were acquired by fitting the data with a nonlinear least-squares formula and the Michaelis–Menten equation using the program Origin 7.0. Kinetic constants were the means of at least three independent sets of data, and they were reproducible within ±10%.

Determination of standard reduction potential by redox titration

Redox titrations were carried out by incubating the proteins (1–2 μM) for 3 h at 30 °C in a reaction mixture that containing 200 mM Tris–HCl, pH 7.5, 2 mM EDTA, and variable molar ratios of GSH/GSSG to reach different half-cell potentials (E_h) according to the Nernst equation [26]. Once incubations were complete, the samples were analyzed in nonreducing SDS–PAGE and the respective reduced fractions were estimated by densitometry, using the program LabImage 2.7.2 (Kapelan GmbH). Titration curves were fitted as reduced fraction versus E_h. Standard reduction potentials ($E_{m7.5}$) were determined by means of nonlinear regression of the data according to a logistic model using the program Origin 7.0.

Confocal laser scanning microscopy

T. cruzi epimastigote cells harvested by centrifugation at 500 *g* for 10 min at 23 °C were washed twice with phosphate-buffered saline (PBS; 8 g l^{-1} NaCl, 0.2 g l^{-1} KCl, 1.44 g l^{-1} Na_2HPO_4, 0.24 g l^{-1} KH_2PO_4, pH 7.4) to remove residual medium components. Cells were fixed with 4% (v/v) paraformaldehyde and permeabilized for 1 h at room temperature in PBS with the addition of 0.05% (v/v) Triton X-100 and 3% (w/v) BSA. Cells were incubated for 1 h at 37 °C with rabbit polyclonal anti-*Tcr*MSR10 antibodies diluted 1/100. Then, they were incubated with a goat anti-rabbit secondary antibody labeled with fluorescein isothiocyanate (FITC; final dilution of 1/1000; ICN Biomedical) for 1 h at 37 °C. Confocal images were collected using a Zeiss LSM5 Pascal laser scanning confocal microscope equipped with an argon/helium/neon laser and a 100× (numerical aperture 1.4) oil immersion objective (Zeiss Plan–Apochromat). Twenty to thirty-five confocal sections of 0.5 μm were taken parallel to the coverslip (*z* sections). Images were acquired using a Zeiss charge-coupled device camera and processed with LSM and ImageJ software. Three-dimensional deconvolution was performed with Autodeblur version 9.3 software. Maximum intensities of five to seven *z* sections were projected into images that depict 3–4 μm of the total *z* stack.

Overexpression of TcrMSR10 in T. cruzi epimastigote cells

The *tcrmsr10* gene was cloned into the pTEX plasmid [27] between the *Bam*HI and the *Hin*dIII restriction sites to generate the recombinant construct (pTEX/*Tcr*MSR). The construct pTEX/GFP was generated by subcloning the *gfp* gene into pTEX for use as a transformation control. The green fluorescence protein (GFP)-encoding gene was obtained from the pNUS-GFP plasmid [28]. *T. cruzi* epimastigote cells were transfected by electroporation according to previous work [27]. Transfected cells were selected by gradually increasing the concentration of the G418 (Invitrogen) until a final concentration of 500 μg ml^{-1} was reached in 4 weeks. The success of the transformation assay was corroborated along with time, by following the augmentation in the number of fluorescent parasites (transfected with the construct pTEX/GFP). Transfected cells were maintained by successive passages in LIT medium (at 28 °C) supplemented with 10% (v/v) bovine fetal serum, 20 μg ml^{-1} hemin, and 500 μg ml^{-1} G418.

Hydrogen peroxide sensitivity experiments

Recombinant *T. cruzi* epimastigotes taken at the logarithmic phase of growth were inoculated (at a cellular density of 10^6 cells ml^{-1}) in multiwell plates with 1 ml of LIT medium supplemented with 10% (v/v) bovine fetal serum, 20 μg ml^{-1} hemin, and 500 μg ml^{-1} G418 and various concentrations of H_2O_2. After 2 days of culture at 28 °C, the cellular density was determined by counting in a Neubauer chamber. The concentration of H_2O_2 that inhibits 50% of parasites growing (IC_{50}) was determined by applying nonlinear regression to the data, using the program Origin 7.0.

Molecular modeling

Structural models were generated by homology modeling using the program Modeller version 9.5 [29], with structure optimization algorithms. Models were based on the resolved structure of MSRA from *Populus trichocarpa* (PDB 2J89), *Bos taurus* (PDB 1FVG), and *M. tuberculosis* (PDB 1NWA). Sequence alignment was carried out using the ClustalX algorithm with the program Bioedit version 7.0.8 (Ibis

Bioscience, 2007). The structures were evaluated using the online program Verify 3D (http://nihserver.mbi.ucla.edu/Verify_3D/), and the program Deep View/Swiss PDB viewer version 4.0 (www.expasy.org/spdbv) was utilized for visualization of the models.

Results

Identification, cloning, and expression of MSR genes from T. cruzi and T. brucei

In the database of the *T. cruzi* genome project (Pathogen Sequencing Unit, Sanger Institute, Wellcome Trust; http://www.genedb.org/) we identified two sequences putatively encoding the respective isoforms of MSRA, *Tcr*MSR10 (Tc00.1047053510855.10) and *Tcr*MSR180 (Tc00.1047053509611.180). In addition, one spliced nucleotide sequence encoding a putative MSRA was found in the database of the *T. brucei* (*Tbr*MSR, Tb08.12O16.110). This information prompted us to perform the molecular cloning of the full-length ORFs for these enzymes. Full-length DNA fragments were amplified by PCR as described under Materials and methods, and their identities were confirmed by DNA sequencing. The three enzymes possess a deduced molecular mass of ca. 20 kDa (in silico). Fig. 1 shows an alignment of the amino acid sequences of *Tcr*MSR10, *Tcr*MSR180, *Tbr*MSR, and MSRA from other organisms. The alignment illustrates the high identity found between these proteins, particularity between *Tcr*MSR10 and *Tcr*MSR180 (96% identity). All the sequences aligned in Fig. 1 contain the redox-active motif GCFWG, which is characteristic of this type of enzyme [10,30].

Genes encoding *Tcr*MSR10, *Tcr*MSR180, and *Tbr*MSR were cloned into pRSET-A and expressed in *E. coli* BL21(DE3) cells as a recombinant protein with a His tag in their N-terminus. Soluble fractions were purified chromatographically, to obtain MSRs with purity higher than 97%, as judged by SDS–PAGE (data not shown). The molecular mass revealed for each protein (≈23 kDa) agrees with the expected size deduced from their DNA-derived amino acid sequence, plus ca. 3 kDa of the His tag found at the N-terminus.

Biological functionality of TcrMSR10, TcrMSR180, and TbrMSR

As shown in Fig. 2, the electrophoretic profiles of MSRs in nonreducing SDS–PAGE were modified after incubation of the enzyme with a reducing agent [such as dithiothreitol (DTT)] or an oxidant (L-MetSO). The oxidized enzyme showed a higher electrophoretic migration compared with the reduced form. The behavior of the oxidized enzymes seems to indicate the formation of an intrachain disulfide bridge, as already evidenced for other MSRAs [4]. L-MetSO is a highly specific chemical oxidant, from which this enzyme–substrate interaction assay strongly supports the functionality of the recombinant MSRs. In addition, we investigated the capacity of *Tcr*TXNI to interact with MSRs. As shown in Fig. 2, either DTT or prereduced *Tcr*TXNI (molecular mass 17 kDa) reverts the oxidation state of *Tcr*MSR10, *Tcr*MSR180, or *Tbr*MSR, thus decreasing their respective electrophoretic mobility. These results confirm the functionality, as a redox couple, of

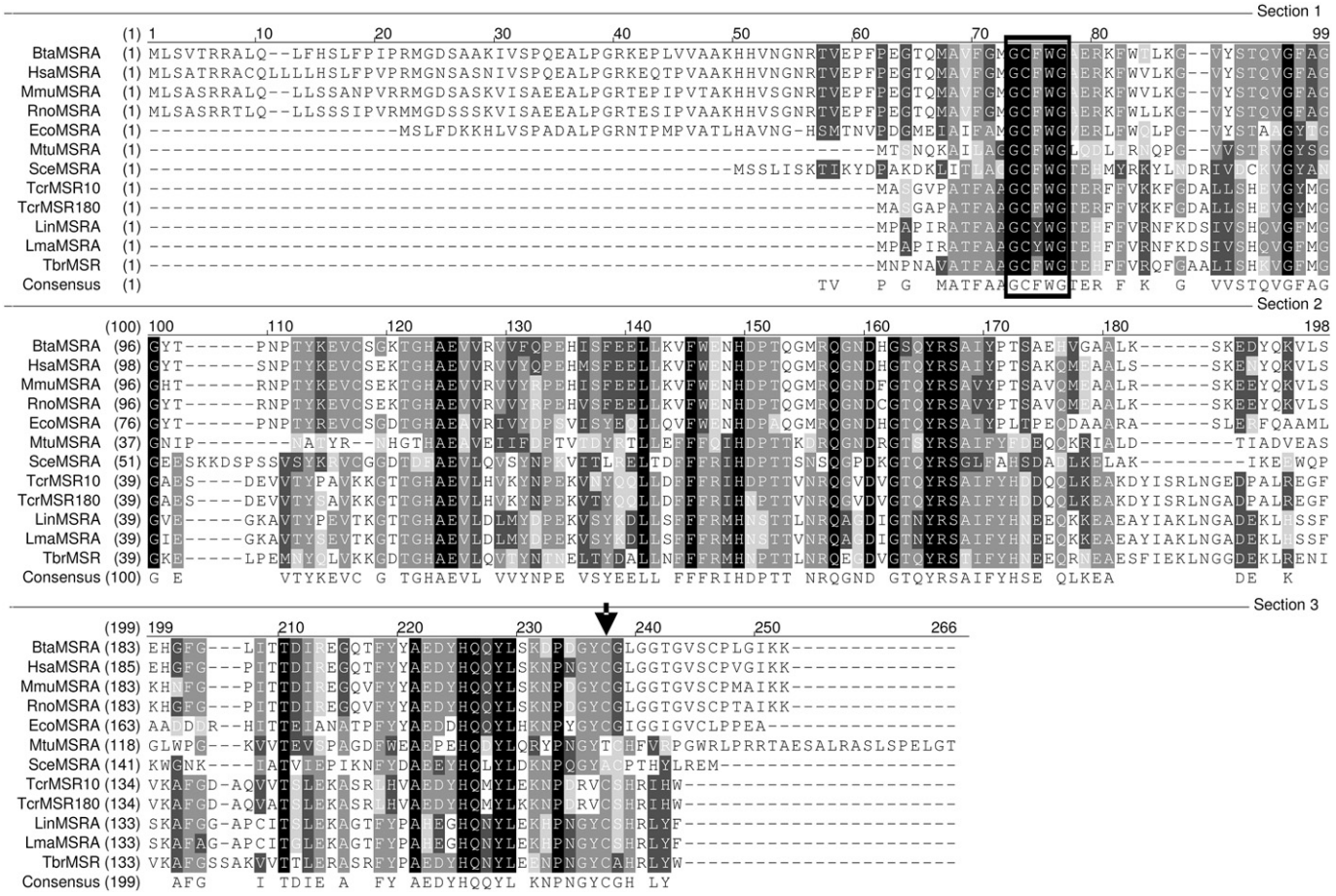

Fig. 1. Amino acid sequence alignment of TcrMSR10, TcrMSR180, and TbrMSR with MSRA homologues. *B. taurus* (NCBI Accession No. AAI02981), *Homo sapiens* (NCBI Accession No. NP_036463), *Mus musculus* (NCBI Accession No. AAH14738), *Rattus norvegicus* (NCBI Accession No. AAH87009), *E. coli* (NCBI Accession No. AAA97115), *M. tuberculosis* (NCBI Accession No. P0A5L0), *Saccharomyces cerevisiae* (NCBI Accession No. NP_010960), *Leishmania infantum* (NCBI Accession No. XP_001470311), and *Leishmania major* (NCBI Accession No. XP_001681026) are shown. Each sequence is numbered accordingly. The black box indicates the redox-active motif and the arrow shows the resolutive cysteine (the residue involved in attacking the sulfenic intermediate during the catalytic cycle, see [4]).

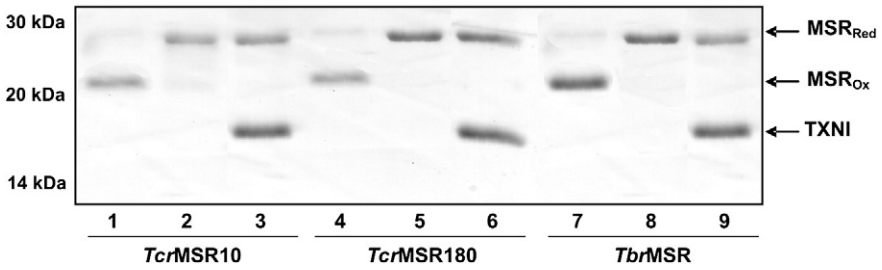

Fig. 2. Reduction assay of MSRs by TcrTXNI visualized by nonreducing SDS–PAGE. *Tcr*MSR10, *Tcr*MSR180, or *Tbr*MSR (4 μM each) were oxidized with 1 mM L-MetSO (lanes 1, 4, and 7). The oxidized proteins were later incubated for 10 min at 37 °C with 1 mM DTT (lanes 2, 5, and 8) or 5 μM *Tcr*TXNI (lanes 3, 6, and 9).

TXN/MSR, suggesting a possible specific interaction between the physiological reducing substrate and the enzyme in vivo.

Steady-state kinetic characterization of MSR

Kinetic studies of trypanosomatid MSR were performed evaluating the reduction of L-MetSO by MSR coupled to NADPH oxidation [4]. In this coupled system, the rate of L-MetSO reduction was dependent on the MSR concentration, *Tcr*TXNI being an essential reducer substrate (data not shown). These results confirm that MSRs have *Tcr*TXNI as a necessary mediator for the electron transfer, which supports a new physiological function for *Tcr*TXNI in the parasite. In addition, the enzymes were specific for L-Met(*S*)SO reduction, not being able to employ L-Met(*R*)SO as a substrate (data not shown), in agreement with reports of MSRA from other sources [31].

Under steady-state kinetics, as occurred with MSRs from different species [31], double reciprocal plots for initial velocities with variable L-Met(*S*)SO concentrations at different fixed values of *Tcr*TXNI yielded parallel lines indicating that the enzyme follows a "ping–pong" or double-substitution mechanism (data not shown). These studies showed that the enzymes exhibit different kinetic profiles. *Tcr*MSR10 and *Tbr*MSR presented Michaelis–Menten kinetics in relation to *Tcr*TXNI and L-Met(*S*)SO, whereas *Tcr*MSR180 showed no saturation kinetics for the same substrates (*Tcr*TXNI and L-Met(*S*)SO). Our results are similar to those of previous reports for MSR from other sources that present no saturation kinetics for the reduction by DTT [31,32]. Kinetic parameters for recombinant MSRs are presented in Table 1. As mentioned previously, these enzymes exhibit a ping–pong mechanism, which can be described in two independent semireactions:

$$MSR_{Red} + L\text{—}MetSO \xrightarrow{k'_1} MSR_{Ox} + L\text{—}Met + H_2O$$

$$MSR_{Ox} + TXNI\text{—}(SH)_2 \xrightarrow{k'_2} MSR_{Red} + TXNI\text{—}S_2$$

Both *Tcr*MSR10 and *Tbr*MSR exhibited pseudo-second-order constants (k'_1) higher than that of *Tcr*MSR180 (100- and 1000-fold, respectively) for the reduction of the sulfoxide (Table 1). Probably, differences in the amino acid residues between *Tcr*MSR180 and the other two enzymes could modify both the binding of the sulfoxide to the enzyme and the catalytic process. However, such a difference does not interfere with the interaction between the enzymes and *Tcr*TXNI, because trypanosomatid MSRs presented similar catalytic efficiencies for oxidation of $TcrTXNI_{Red}$ (Table 1). For the three enzymes, calculated k'_2 were higher than that observed for the reduction of L-Met(*S*)SO. Variations in the ionic strength did not significantly affect the activity of MSRAs. In addition, profiles of activity with pH showed an optimal rank of pH between 7.0 and 7.5 (data not shown). Interestingly, we observed the absence of MSR inhibition by L-Met, even at 400-fold excess of the latter with respect to L-MetSO. This might indicate a low affinity of MSRs for L-Met or could also indicate an irreversibility of the catalyzed reaction.

Table 1
Kinetic parameters of recombinant MSRs, determined at 30 °C and pH 7.5

Enzyme	Substrate	k_{cat} (min^{-1})	K_m (μM)	$k_{cat}\,K_m^{-1}$ ($M^{-1}\,s^{-1}$)
*Tcr*MSR10	L-Met(*S*)SO	31	723	7.2×10^2 (k'_1)
*Tcr*MSR10	*Tcr*TXNI	31	33	1.8×10^4 (k'_2)
*Tcr*MSR180	L-Met(*S*)SO	ND	ND	8.6 (k'_1)[a]
*Tcr*MSR180	*Tcr*TXNI	ND	ND	7.7×10^4 (k'_2)[a]
*Tbr*MSR	L-Met(*S*)SO	19	69	4.6×10^3 (k'_1)
*Tbr*MSR	*Tcr*TXNI	19	13	2.4×10^4 (k'_2)

Assays were performed as detailed under Materials and methods at various concentrations of substrate in the range 20–2500 μM L-Met(*S*)SO and 0.5–20 μM *Tcr*TXNI. ND, not determinable because of absence of saturation.

[a] Calculated from the slope of the secondary graph: $V_{m\ app}$ vs [*Tcr*TXNI].

Redox titration of trypanosomatid MSRs

Thermodynamic properties of recombinant MSRs were evaluated after incubation of the purified enzymes with various GSH/GSSG ratios, followed by nonreducing SDS–PAGE and densitometry to determine the relative amounts of oxidized and reduced forms of the respective enzyme. With the data obtained we constructed graphs of reduced fraction vs E_h (generated for each combination of GSH/GSSG at 30 °C and pH 7.5). Fig. 3A depicts the profile of bands for each protein at the various GSH/GSSG ratios. From titration curves (Fig. 3B), we determined $E_{m7.5}$ of -176 ± 5 mV for *Tcr*MSRS10, -178 ± 5 mV for *Tcr*MSR180, and -189 ± 9 mV for *Tbr*MSR. These redox potentials were similar, thus indicating that discrepancies observed in the kinetic properties would not depend on differences in redox capacities (reactivity) of cysteine residues participating in the catalytic cycle in these enzymes.

Trypanosomatid MSRs are monomeric proteins and present different surface charge distributions

Measurement of molecular mass for recombinant *Tcr*MSR10, *Tcr*MSR180, and *Tbr*MSR under various redox conditions allowed us to determine that the proteins are monomers independent of their redox state (Fig. 4). Fig. 4A shows electrophoretic profiles for the proteins in the reduced and oxidized state. It can be observed that *Tcr*MSR180 exhibited slower migration than *Tcr*MSR10 or *Tbr*MSR. Fig. 4B (inset) shows parallel lines in semilogarithm plots of relative electrophoretic mobility (log *U*) for each protein vs the gel concentration (%*T*), which indicate that the proteins (in their reduced or oxidized forms) have the same molecular mass [33]. Using the values of K_D (slopes) obtained from the Ferguson primary graph for each MSR, we estimated a molecular mass of 24 kDa for *Tcr*MSR10, 30 kDa for *Tcr*MSR180, and 23 kDa for *Tbr*MSR (Fig. 4B). These masses correlate with a monomeric structure, similar to that found for other orthologues [34,35]. In contrast, we observed a marked difference in the *y*-intercept of this graph for *Tcr*MSR10, *Tbr*MSR, and *Tcr*MSR180.

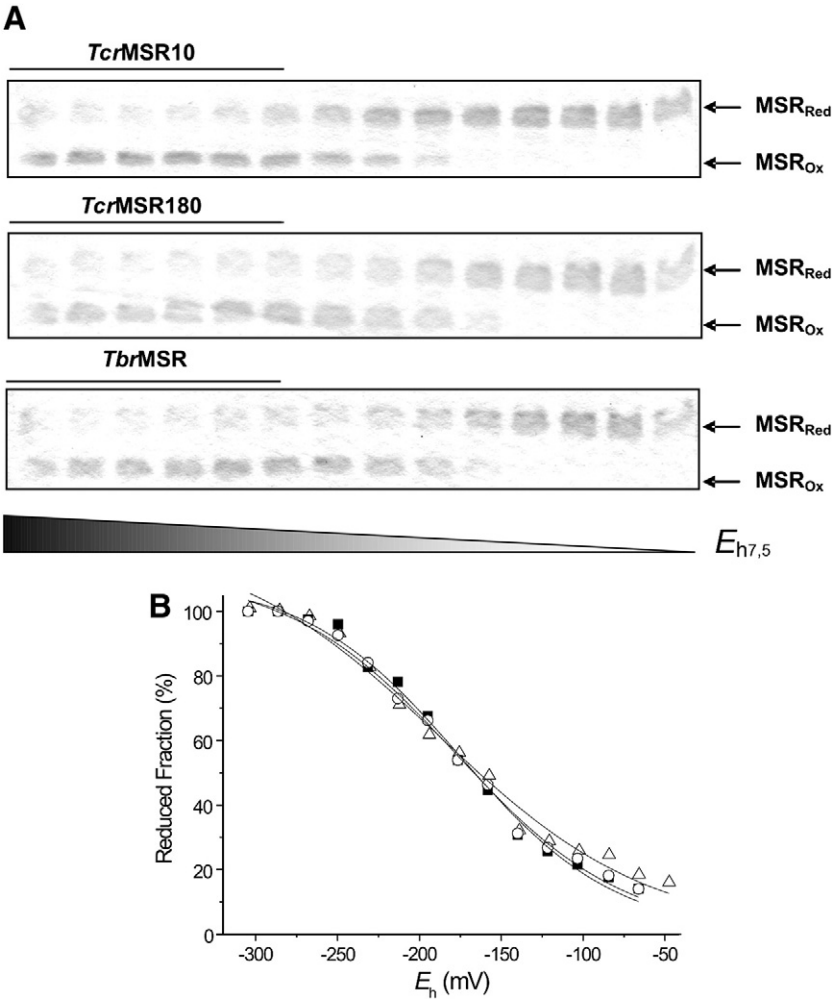

Fig. 3. Redox titration of trypanosomatid MSRs. (A) Nonreducing SDS–PAGE profiles of MSRs incubated at 30 °C and pH 7.5 with various GSH/GSSG ratios for 4 h. (B) Redox titration curves of (■) *Tcr*MSR10, (○) *Tcr*MSR180, and (△) *Tbr*MSR.

The value of the *y*-intercept is the logarithm of the free electrophoretic mobility (U_L), which is related to the superficial charge distribution of the protein to a certain pH. We inferred that *Tcr*MSR180 has a smaller value of free electrophoretic mobility than *Tcr*MSR10 or *Tbr*MSR, which might indicate that the former protein has a less negative net charge under the experimental conditions (pH 8.8). This effect is correlated with in silico predicted p*I* values for trypanosomatid MSRAs, showing significant differences: 6.14 for *Tcr*MSR10, 5.98 for *Tbr*MSR, and 7.28 for *Tcr*MSR180. Consequently, differences observed in the electrophoretic migration could be attributed to dissimilar superficial charge profiles exhibited by the proteins, rather than to variations in molecular masses. Differences observed in the reactivity (activity) toward substrates of MSRs under study could be due to distinctive superficial charge profiles characteristic of each protein, as analyzed in silico by molecular modeling (Fig. 5). These differences could affect the interaction of the enzymes with their substrates. Previous studies [36] reported the relationship between the evolution of electric properties and cellular localization and function of several protein isoforms of vertebrate fructose-1,6-bisphosphate aldolase, RNase I, triose phosphate isomerase, and phosphoglucose isomerase. The authors indicated the existence of possible neofunctionalization after gene duplication. A similar situation might be possible in *T. cruzi*, in which both *Tcr*MSR10 and *Tcr*MSR180 differ in electrical and kinetic properties, which could be ascribed to an established specific cellular localization to functionality dependence for these proteins [36].

Evaluation of MSR expression in various forms of T. cruzi and T. brucei

The expression of MSR in various stages of both *T. cruzi* and *T. brucei* was evaluated in a Western blot assay using a polyclonal anti-*Tcr*MSR10 serum and total extracts from *T. cruzi* and *T. brucei*. As shown by Fig. 6A, in *T. cruzi* positive signals were detected only in extracts from epimastigotes and amastigotes (both replicative stages) and not in the nonreplicative form (trypomastigote). Positive signals were detected on both procyclic and bloodstream stages in *T. brucei* (Fig. 6B). The presence of MSR was further characterized by performing cellular immunolocalization of *Tcr*MSR in *T. cruzi* epimastigote cells, using polyclonal anti-*Tcr*MSR10 antibodies (Fig. 7). The images obtained, by either epifluorescence (Fig. 7A) or confocal (Fig. 7B) microscopy, revealed recognition signals distributed in the whole parasite cell. This would indicate a cytoplasmic location of at least one of the isoforms. Results are consistent with previous reports on the cellular location of MSR in other organisms [37].

Overexpression of TcrMSR10 in epimastigote cells confers resistance to oxidative stress

T. cruzi epimastigote cells were transfected with either the recombinant construct (pTEX/*Tcr*MSR) or the empty vector (pTEX) to evaluate further the functions of MSR in trypanosomatids. Afterward successive passages of the cell lines in fresh medium (supplemented

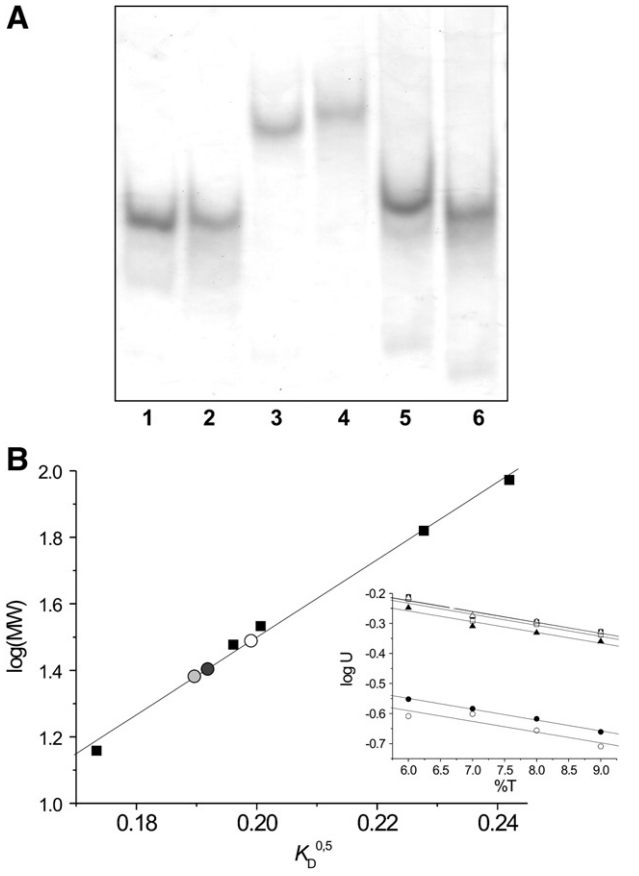

Fig. 4. Determination of native molecular masses of MSRs. A) Proteins were resolve by 6% native PAGE stained with Coomassie blue in different conditions. Lane 1, *Tcr*MSR10 incubated with 10 mM DTT; lane 2, *Tcr*MSR10 incubated with 10 mM L-MetSO; lane 3, *Tcr*MSR180 incubated with 10 mM DTT; lane 4, *Tcr*MSR180 incubated with 10 mM L-MetSO; lane 5, *Tbr*MSR incubated with 10 mM DTT; and lane 6, TbrMSR incubated with 10 mM L-MetSO. B) Secondary Ferguson plot was generated by plotting the root square of retardation coefficient vs. the masses of the molecular weight markets (■). The retardation coefficient calculated for *Tcr*MSR10, *Tcr*MSR180 and *Tbr*MSR were 0.0360 (○), 0.0403 (●) and 0.0365 (⊠), respectively. Inset: Primary Ferguson plot of (■) *Tcr*MSR10 incubated with 10 mM DTT; (□) *Tcr*MSR10 incubated with 10 mM L-MetSO; (●) *Tcr*MSR180 incubated with 10 mM DTT (○); *Tcr*MSR180 incubated with 10 mM L-MetSO; (▲) *Tbr*MSR incubated with 10 mM DTT and (△) *Tbr*MSR incubated with 10 mM L-MetSO.

with G418) were carried out for 60 days until complete selection of the cellular lines. Epimastigote forms of *T. cruzi* transfected with pTEX/*Tcr*MSR did not exhibit significant differences in morphology or growth

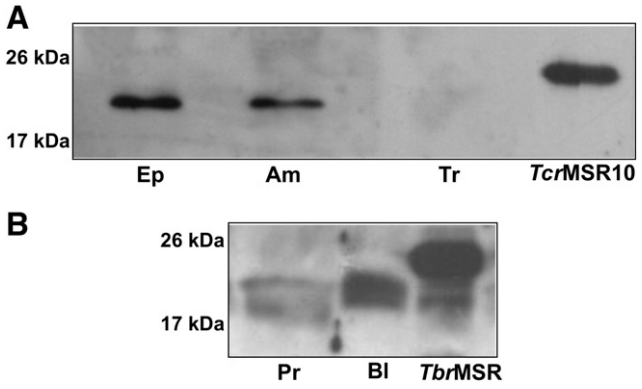

Fig. 6. Immunodetection of MSR in different stages of *T. cruzi* and *T. brucei*. Approximately 40 μg of protein extracts was separated by 15% SDS–PAGE and transferred to nitrocellulose membranes. Blots were probed with anti-*Tcr*MSR10 and with preimmune serum (data not shown). (A) Protein extracts from *T. cruzi* epimastigote (Ep), amastigote (Am), and trypomastigote (Tr) cells. (B) Protein extracts from *T. brucei* procyclic (Pr) and bloodstream (Bl) cells. As marker control, 50 ng of His-tagged recombinant *Tcr*MSR10 or *Tbr*MSR was used.

rate with respect to the controls (data not shown). Immunological analysis (Western blot) verified the high level of expression of the protein (between 15- and 20-fold) in the transfected cellular line (Fig. 8A). We determined that the overexpression of *Tcr*MSR10 in *T. cruzi* conferred resistance to oxidative stress, as transfected cells exhibited around 2-fold more tolerance to exogenous H_2O_2, presenting an IC_{50} of 141 ± 6 μM. The control cell line (transfected with empty vector pTEX) exhibited an IC_{50} of 76 ± 3 μM. The observed difference in IC_{50} values was statistically significant ($p = 0.039$ with $n = 3$), as evaluated by Student's *t* test (Fig. 8B). Similar behavior was reported by other authors who have studied the overexpression of different proteins belonging to the antioxidant mechanisms in *T. cruzi* [21,38].

Discussion

T. cruzi and *T. brucei* are the etiologic agents of Chagas and sleeping sickness disease, respectively, which constitute two main problems for public health in Latin America and Africa (WHO; http://www.who.int/es/). In trypanosomatids, the study of antioxidant systems has been widely settled on the central role played by trypanothione in the redox metabolism in these organisms [39]. It is clear that the ability of these pathogens to resist oxidative stress is essential for survival during the infection of mammalian tissues [40]. Currently, there is a general understanding about the mechanisms responsible for this resistance, but the characterization of the various actors in redox

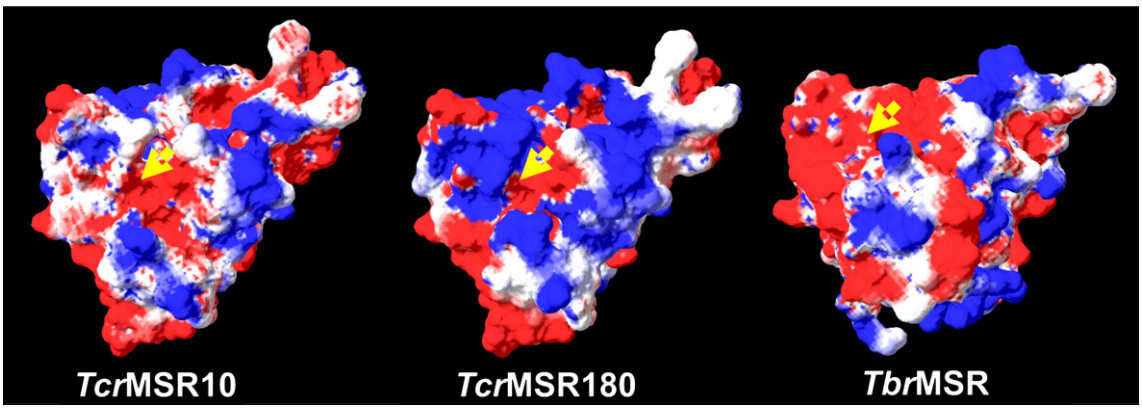

Fig. 5. Electrostatic potential of MSRs. Electrostatic potential on the molecular surface predicted by the molecular model (generated as detailed under Materials and methods) was calculated using the Poisson–Boltzmann equation with the Swiss-pdb viewer version 4.0 program. As conditions for the calculation we used a dielectric constant value of 80, a dielectric constant value of the protein of 4, and an ionic strength of 0.0 mol l^{-1}. The positive charges are represented in blue and the negative charges are represented in red. The arrows indicate the active sites of the proteins.

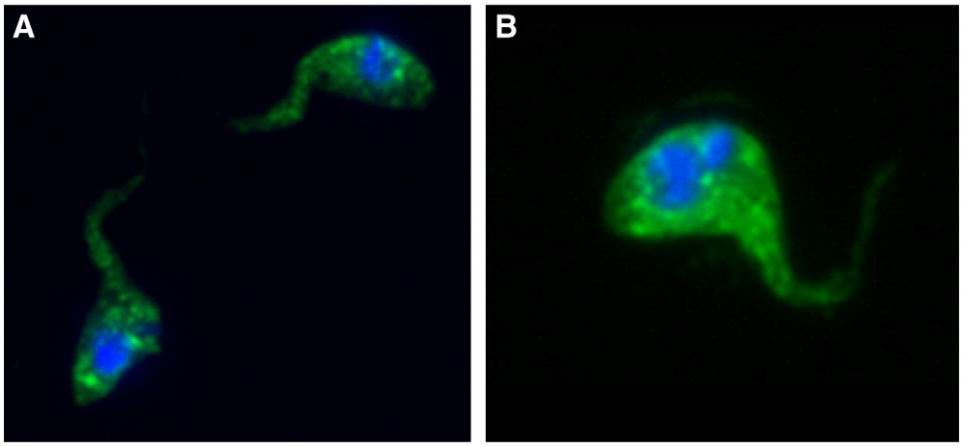

Fig. 7. Immunolocalization of *Tcr*MSR in *T. cruzi* epimastigote cells. (A) Epifluorescence microscopy using rabbit polyclonal anti-*Tcr*MSR10 antibodies and FITC-conjugated goat anti-rabbit antibody. The fluorescent nuclear staining was performed with DAPI. (B) Confocal laser scanning microscopy of epimastigote cells of *T. cruzi* CL-Brener using polyclonal anti-*Tcr*PMSR10 antibodies. The images of the cellular location of *Tcr*MSR show an intense mark at cytoplasmic level (3.8 μm depth). Controls were performed using only the FITC-conjugated antibody, not presenting a recognition signal (not shown).

metabolism is still far from being completed. Thus, for trypanosomatids there is no information about the mechanisms for repairing oxidized proteins and their relevance for the survival of these pathogens in the various stages of their life cycle.

The *T. cruzi* and *T. brucei* genome projects offer information on nucleotide sequences encoding MSRA in both parasites. In this work we present the cloning, expression, and characterization of three MSRAs from trypanosomatids. To the best of our knowledge, this is the first detailed study of this type of enzyme from parasitic protozoa. Our kinetic and electrophoretic data indicate that the reduction of L-MetSO by trypanosomatid MSRs followed a mechanism of formation/rupture of an intramolecular disulfide bridge. Because in the primary structure of each of these proteins only two cysteinyl residues are found (Cys^{13} and Cys^{171}), it can be speculated that they are involved in the mechanism.

The reversion from the oxidized state of recombinant MSRAs was dependent on the presence of reduced TXN, a potential physiological reducing substrate of MSRs. Thus, our results not only indicate that the recombinant MSRs were biologically active but they also strongly support a new redox pathway in trypanosomatids, with the participation of different physiological substrates.

Results of the steady-state kinetics verified that the characterized MSRs have a double-substitution reaction mechanism, which is a common kinetic mechanism for this kind of enzyme [31]. Our studies reveal different kinetic behavior between the MSRAs from *T. cruzi* and *T. brucei.* Thus, *Tcr*MSR10 and *Tbr*MSR showed saturation kinetics, whereas *Tcr*MSR180 did not. As was previously mentioned, both types of kinetics have been reported for MSR from other sources [32]. Similarities and differences found for the calculated pseudo-second-order constants (k') for both reduction/oxidation reactions would explain dissimilarities observed in the enzymatic activity. These results seem to indicate that, in all cases, the reduction of L-MetSO is the slow reaction in the catalytic cycle. This behavior is similar to that reported for MSRA from *E. coli* [32], *P. trichocarpa* [41], and *Caenorhabditis elegans* [42], as well as for MSRB from *Neisseria meningitidis* [7], all of them studied by steady-state kinetic analyses.

Redox potentials of the recombinant enzymes from trypanosomatids were similar. Thus, we can consider that the kinetic discrepancies exhibited by *Tcr*MSR10, *Tbr*MSR, and *Tcr*MSR180 should not be a consequence of differences in the redox capacity of the active cysteine residues of the proteins. Values of $E_{m7.5}$ determined for the trypanosomatid MSRs (average value of −181 mV) thermodynamically justify the capacity of these enzymes to use TXN ($E^{\circ\prime}$ of −249 mV for TXN of *T. brucei* [43]) as a reducing substrate. Values of redox potentials determined in this study for MSRs are coherent with a flow of reduction equivalents transported through the trypanothione-dependent system, originally from NADPH ($E^{\circ\prime}$ of −320 mV [43]), to trypanothione ($E^{\circ\prime}$ of −242 mV [43]), and then to the protein thiol. An important property of this type of enzyme is the lack of inhibition by product, particularly by L-Met [4], so the presence of L-Met in the reaction mixture did not show an inhibitory effect, suggesting a low affinity of MSRs for L-Met. In agreement with our results, MSRA from *N. meningitidis* has a K_i value for *N*-acetyl-L-methionine-*N*-methylamide of around 2 M [4].

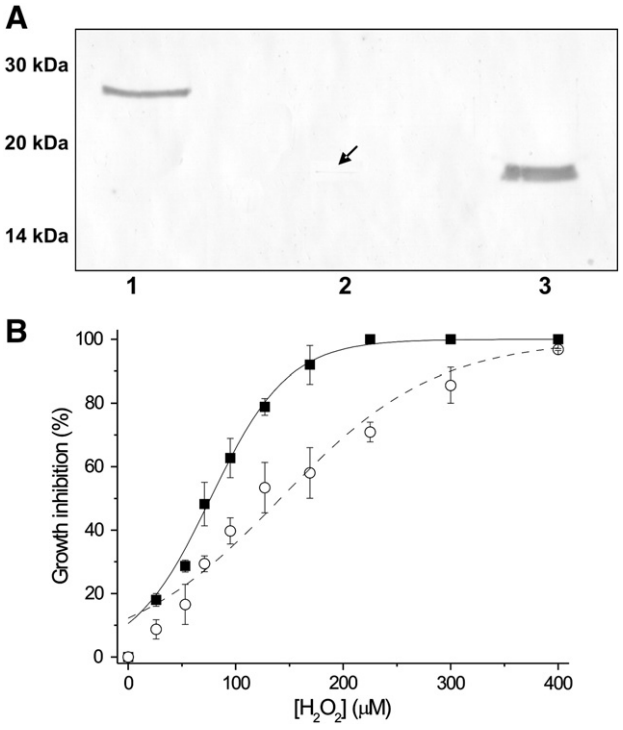

Fig. 8. Overexpression of *Tcr*MSR10 in *T. cruzi* epimastigote cells. (A) Western blot of transfected epimastigote cells of *T. cruzi* CL-Brener. Lane 1, 1 μg of recombinant *Tcr*MSR10; lane 2, crude extract of 8×10^5 parasites transfected with pTEX; and lane 3, crude extract of 8×10^5 parasites transfected with the recombinant construct pTEX/*Tcr*MSR10. The bands were revealed using polyclonal anti-*Tcr*MSR10 antibodies. (B) Susceptibility of recombinant epimastigote cells of *T. cruzi* to H_2O_2. Parasites were transfected with (■)the pTEX plasmid or (○) the recombinant construct pTEX/*Tcr*MSR and then cultivated in the presence of various concentrations of H_2O_2. After 48 h of incubation, the cellular density was determined by counting in a Neubauer chamber. A p value of 0.039 was obtained for the difference in the growth inhibition curve between the two strains.

The collected data reveal that MSRAs from trypanosomatids have a monomeric structure with a molecular mass between 24 and 30 kDa; nevertheless they exhibit different mobilities in native electrophoresis. The odd mobility characteristics probably originated from differences in the distribution of superficial charge. Our hypothesis is coherent with p*I* values predicted in silico for each MSR, which suggests that at working pH (pH 8.8), both *Tcr*MSR10 and *Tbr*MSR would have more superficial negative charge than *Tcr*MSR180 and so a greater electrophoretic mobility. On the other hand, even when these proteins have a high structural similarity (as deduced from molecular modeling), they seem to have a remarkable difference at the level of superficial charge profile. Using the Poisson–Boltzmann equation [44], we calculated that *Tcr*MSR180 is more electropositive than *Tcr*MSR10 and *Tbr*MSR. These theoretical results were correlated with those experimentally obtained by native PAGE procedures.

Although differences found in the electrostatic properties of the enzymes could be responsible for variations in the kinetic parameters of these proteins, the binding of L-MetSO to the enzyme was not affected, because critical residues involved in such a function are highly conserved in all the enzymes. Electrostatic properties of MSRs could kinetically affect both the attack on the sulfoxide by the thiol of Cys^{13} (formation of a sulfenic group) and the later reduction of this sulfenic group by the resolutive Cys^{171} for making a disulfide bridge. This hypothesis is based on: (i) the 100-fold difference observed between pseudo-second-order kinetic constants for the reduction of the sulfoxide corresponding to *Tcr*MSR10/*Tbr*MSR and *Tcr*MSR180 and (ii) the similarity found between the kinetic constants for the reaction between the MSR_{Ox} and *Tcr*$TXNI_{Red}$. This would indicate a priori that the superficial electrostatic properties in *Tcr*MSR180 cause a slower sulfoxide reduction compared with *Tcr*MSR10 or *Tbr*MSR. The specific substrate for *Tcr*$TXNI_{Red}$ would be the disulfide bridge of the MSR_{Ox} rather than the sulfenic group of the Cys^{13} (intermediary reaction in the reduction of L-MetSO) [4]. This agrees with existing reports in the literature [45,46] about other protein thiols like TRX. This supports that the reaction between *Tcr*$TXNI_{Red}$ and MSR_{Ox} would be possible only after the existence of a disulfide bridge in these enzymes (oxidized form).

The expression of at least one of the genes encoding *Tcr*MSR in *T. cruzi* was confirmed by Western blot, obtaining positive signals only in the parasite replicative stages (epimastigote and amastigote), whereas *Tbr*MSR is expressed in both stages of *T. brucei* (procyclic and bloodstream). Our study on the cellular immunolocalization in *T. cruzi* by confocal microscopy detected MSRA with a cytoplasmic location in epimastigote cells. We analyzed the overexpression of *Tcr*MSR10 in epimastigote cells of *T. cruzi* and determined that it conferred increased (approximately twofold with respect to the control) tolerance to oxidative stress generated by exogenous H_2O_2. Other authors have reported similar increases in the resistance to oxidant conditions after overexpression assays of glutathione peroxidase I [21], ascorbate peroxidase [38], TR [47], and cytoplasmic and mitochondrial peroxiredoxins [40,48]. Our findings strongly support a key function of MSRAs in the redox metabolism of trypanosomatids. The overall picture leads us to conclude that in *T. cruzi,* as well as in *T. brucei,* MSRs might help the parasites to cope with oxidative stress. These enzymes do not participate in a direct elimination of oxidant agents, but in repairing oxidized proteins for maintaining a correct cellular functionality. Similar results have been obtained after overexpression of MSRA in *E. coli* cells [49], MSRB in *Arabidopsis thaliana* [6], or MSRB in mammalian cell cultures [50], where the transformed cells exhibited enhanced tolerance to abiotic stress. Finally, this is the first time that a functional system responsible for the repair of oxidized proteins has been described in both *T. cruzi* and *T. brucei.* That adds value to the genome project of these parasites. Our data suggest that this new metabolic pathway could be an important tool for the regulation of the functionality of metabolic routes involving enzymes containing critical Met residues and encourage us to follow the in-depth characterization of these and other putative macromolecules, in these parasites, working together with MSRA in the reduction of MetSO. In this context, TXNI emerges as a redox molecule playing new specific roles in the metabolic machinery of the parasite.

Acknowledgments

This work was supported by grants from UNL (CAI+D Orientados & Redes), CONICET (PIP 112 2008-01-02519), and ANPCyT (PICT'07 668). D.G.A., E.D.E., and P.G.C. are Fellows of CONICET. M.S.C. is a Fellow of ANPCyT. A.A.I., H.D.L., M.T.T.I., and S.A.G. are Investigator Career Members of CONICET.

References

[1] Nordberg, J.; Arner, E. S. Reactive oxygen species, antioxidants, and the mammalian thioredoxin system. *Free Radic. Biol. Med.* **31:**1287–1312; 2001.
[2] Moskovitz, J. Methionine sulfoxide reductases: ubiquitous enzymes involved in antioxidant defense, protein regulation, and prevention of aging-associated diseases. *Biochim. Biophys. Acta* **1703:**213–219; 2005.
[3] Friguet, B. Oxidized protein degradation and repair in ageing and oxidative stress. *FEBS Lett.* **580:**2910–2916; 2006.
[4] Boschi-Muller, S.; Gand, A.; Branlant, G. The methionine sulfoxide reductases: catalysis and substrate specificities. *Arch. Biochem. Biophys.* **474:**266–273; 2008.
[5] Moskovitz, J.; Flescher, E.; Berlett, B. S.; Azare, J.; Poston, J. M.; Stadtman, E. R. Overexpression of peptide-methionine sulfoxide reductase in Saccharomyces cerevisiae and human T cells provides them with high resistance to oxidative stress. *Proc. Natl Acad. Sci. USA* **95:**14071–14075; 1998.
[6] Bechtold, U.; Murphy, D. J.; Mullineaux, P. M. Arabidopsis peptide methionine sulfoxide reductase2 prevents cellular oxidative damage in long nights. *Plant Cell* **16:**908–919; 2004.
[7] Olry, A.; Boschi-Muller, S.; Marraud, M.; Sanglier-Cianferani, S.; Van Dorsselear, A.; Branlant, G. Characterization of the methionine sulfoxide reductase activities of PILB, a probable virulence factor from Neisseria meningitidis. *J. Biol. Chem.* **277:** 12016–12022; 2002.
[8] Moskovitz, J.; Singh, V. K.; Requena, J.; Wilkinson, B. J.; Jayaswal, R. K.; Stadtman, E. R. Purification and characterization of methionine sulfoxide reductases from mouse and Staphylococcus aureus and their substrate stereospecificity. *Biochem. Biophys. Res. Commun.* **290:**62–65; 2002.
[9] Lee, W. L.; Gold, B.; Darby, C.; Brot, N.; Jiang, X.; de Carvalho, L. P.; Wellner, D.; St John, G.; Jacobs Jr., W. R.; Nathan, C. Mycobacterium tuberculosis expresses methionine sulphoxide reductases A and B that protect from killing by nitrite and hypochlorite. *Mol. Microbiol.* **71:**583–593; 2009.
[10] Moskovitz, J.; Poston, J. M.; Berlett, B. S.; Nosworthy, N. J.; Szczepanowski, R.; Stadtman, E. R. Identification and characterization of a putative active site for peptide methionine sulfoxide reductase (MsrA) and its substrate stereospecificity. *J. Biol. Chem.* **275:**14167–14172; 2000.
[11] Krauth-Siegel, R. L.; Comini, M. A. Redox control in trypanosomatids, parasitic protozoa with trypanothione-based thiol metabolism. *Biochim. Biophys. Acta* **1780:**1236–1248; 2008.
[12] Irigoin, F.; Cibils, L.; Comini, M. A.; Wilkinson, S. R.; Flohe, L.; Radi, R. Insights into the redox biology of *Trypanosoma cruzi:* trypanothione metabolism and oxidant detoxification. *Free Radic. Biol. Med.* **45:**733–742; 2008.
[13] El-Sayed, N. M.; Myler, P. J.; Bartholomeu, D. C.; Nilsson, D.; Aggarwal, G.; Tran, A. N.; Ghedin, E.; Worthey, E. A.; Delcher, A. L.; Blandin, G.; Westenberger, S. J.; Caler, E.; Cerqueira, G. C.; Branche, C.; Haas, B.; Anupama, A.; Arner, E.; Aslund, L.; Attipoe, P.; Bontempi, E.; Bringaud, F.; Burton, P.; Cadag, E.; Campbell, D. A.; Carrington, M.; Crabtree, J.; Darban, H.; da Silveira, J. F.; de Jong, P.; Edwards, K.; Englund, P. T.; Fazelina, G.; Feldblyum, T.; Ferella, M.; Frasch, A. C.; Gull, K.; Horn, D.; Hou, L.; Huang, Y.; Kindlund, E.; Klingbeil, M.; Kluge, S.; Koo, H.; Lacerda, D.; Levin, M. J.; Lorenzi, H.; Louie, T.; Machado, C. R.; McCulloch, R.; McKenna, A.; Mizuno, Y.; Mottram, J. C.; Nelson, S.; Ochaya, S.; Osoegawa, K.; Pai, G.; Parsons, M.; Pentony, M.; Pettersson, U.; Pop, M.; Ramirez, J. L.; Rinta, J.; Robertson, L.; Salzberg, S. L.; Sanchez, D. O.; Seyler, A.; Sharma, R.; Shetty, J.; Simpson, A. J.; Sisk, E.; Tammi, M. T.; Tarleton, R.; Teixeira, S.; Van Aken, S.; Vogt, C.; Ward, P. N.; Wickstead, B.; Wortman, J.; White, O.; Fraser, C. M.; Stuart, K. D.; Andersson, B. The genome sequence of Trypanosoma cruzi, etiologic agent of Chagas disease. *Science* **309:**409–415; 2005.
[14] Flohe, L.; Hecht, H. J.; Steinert, P. Glutathione and trypanothione in parasitic hydroperoxide metabolism. *Free Radic. Biol. Med.* **27:**966–984; 1999.
[15] Flohe, L.; Steinert, P.; Hecht, H. J.; Hofmann, B. Tryparedoxin and tryparedoxin peroxidase. *Meth. Enzymol.* **347:**244–258; 2002.
[16] Piacenza, L.; Alvarez, M. N.; Peluffo, G.; Radi, R. Fighting the oxidative assault: the Trypanosoma cruzi journey to infection. *Curr. Opin. Microbiol.* **12:**415–421; 2009.
[17] Gomez, M. L.; Erijman, L.; Arauzo, S.; Torres, H. N.; Tellez-Inon, M. T. Protein kinase C in Trypanosoma cruzi epimastigote forms: partial purification and characterization. *Mol. Biochem. Parasitol.* **36:**101–108; 1989.
[18] Allaoui, A.; Francois, C.; Zemzoumi, K.; Guilvard, E.; Ouaissi, A. Intracellular growth and metacyclogenesis defects in Trypanosoma cruzi carrying a targeted deletion of a Tc52 protein-encoding allele. *Mol. Microbiol.* **32:**1273–1286; 1999.
[19] Andrews, N. W.; Colli, W. Adhesion and interiorization of Trypanosoma cruzi in mammalian cells. *J. Protozool.* **29:**264–269; 1982.

[20] Maniatis, T.; Fritsch, E. F.; Sambrook, J. Molecular Cloning: a Laboratory Manual. Cold Spring Harbor Laboratory, Cold Spring Harbor, NY; 1982.
[21] Wilkinson, S. R.; Meyer, D. J.; Taylor, M. C.; Bromley, E. V.; Miles, M. A.; Kelly, J. M. The Trypanosoma cruzi enzyme TcGPXI is a glycosomal peroxidase and can be linked to trypanothione reduction by glutathione or tryparedoxin. *J. Biol. Chem.* **277:**17062–17071; 2002.
[22] Laemmli, U. K. Cleavage of structural proteins during the assembly of the head of bacteriophage T4. *Nature* **227:**680–685; 1970.
[23] Bradford, M. M. A rapid and sensitive method for the quantitation of microgram quantities of protein utilizing the principle of protein–dye binding. *Anal. Biochem.* **72:**248–254; 1976.
[24] Vaitukaitis, J.; Robbins, J. B.; Nieschlag, E.; Ross, G. T. A method for producing specific antisera with small doses of immunogen. *J. Clin. Endocrinol. Metab.* **33:** 988–991; 1971.
[25] Ferguson, K. A. Starch-gel electrophoresis—application to the classification of pituitary proteins and polypeptides. *Metabolism* **13:**985–1002 (Suppl.); 1964.
[26] Forman, H.; Fukuto, J.; Torres, M. Signal Transduction by Reactive Oxygen and Nitrogen Species: Pathways and Chemical Principles. Kluwer Academic, Dordrecht; 2004.
[27] Kelly, J. M.; Ward, H. M.; Miles, M. A.; Kendall, G. A shuttle vector which facilitates the expression of transfected genes in Trypanosoma cruzi and Leishmania. *Nucleic Acids Res.* **20:**3963–3969; 1992.
[28] Tetaud, E.; Lecuix, I.; Sheldrake, T.; Baltz, T.; Fairlamb, A. H. A new expression vector for Crithidia fasciculata and Leishmania. *Mol. Biochem. Parasitol.* **120:** 195–204; 2002.
[29] Eswar, N.; Webb, B.; Marti-Renom, M. A.; Madhusudhan, M. S.; Eramian, D.; Shen, M. Y.; Pieper, U.; Sali, A. Comparative protein structure modeling using MODELLER. Current Protocols in Protein Science, John Wiley & Sons, Inc., Supplement 15, 5.6.1-5.6.30, University of California at San Francisco, San Francisco, California, USA; 2006.
[30] Kauffmann, B.; Aubry, A.; Favier, F. The three-dimensional structures of peptide methionine sulfoxide reductases: current knowledge and open questions. *Biochim. Biophys. Acta* **1703:**249–260; 2005.
[31] Boschi-Muller, S.; Olry, A.; Antoine, M.; Branlant, G. The enzymology and biochemistry of methionine sulfoxide reductases. *Biochim. Biophys. Acta* **1703:** 231–238; 2005.
[32] Boschi-Muller, S.; Azza, S.; Branlant, G. *E. coli* methionine sulfoxide reductase with a truncated N terminus or C terminus, or both, retains the ability to reduce methionine sulfoxide. *Protein Sci.* **10:**2272–2279; 2001.
[33] Rodbard, D.; Chrambach, A. Unified theory for gel electrophoresis and gel filtration. *Proc. Natl Acad. Sci. USA* **65:**970–977; 1970.
[34] Coudevylle, N.; Antoine, M.; Bouguet-Bonnet, S.; Mutzenhardt, P.; Boschi-Muller, S.; Branlant, G.; Cung, M. T. Solution structure and backbone dynamics of the reduced form and an oxidized form of E. coli methionine sulfoxide reductase A (MsrA): structural insight of the MsrA catalytic cycle. *J. Mol. Biol.* **366:**193–206; 2007.
[35] Taylor, A. B.; Benglis Jr., D. M.; Dhandayuthapani, S.; Hart, P. J. Structure of Mycobacterium tuberculosis methionine sulfoxide reductase A in complex with protein-bound methionine. *J. Bacteriol.* **185:**4119–4126; 2003.
[36] Sato, Y.; Nishida, M. Electric charge divergence in proteins: insights into the evolution of their three-dimensional properties. *Gene* **441:**3–11; 2009.
[37] Moskovitz, J.; Bar-Noy, S.; Williams, W. M.; Requena, J.; Berlett, B. S.; Stadtman, E. R. Methionine sulfoxide reductase (MsrA) is a regulator of antioxidant defense and lifespan in mammals. *Proc. Natl Acad. Sci. USA* **98:**12920–12925; 2001.
[38] Wilkinson, S. R.; Obado, S. O.; Mauricio, I. L.; Kelly, J. M. Trypanosoma cruzi expresses a plant-like ascorbate-dependent hemoperoxidase localized to the endoplasmic reticulum. *Proc. Natl Acad. Sci. USA* **99:**13453–13458; 2002.
[39] Krauth-Siegel, R. L.; Comini, M. A. Redox control in trypanosomatids, parasitic protozoa with trypanothione-based thiol metabolism. *Biochim. Biophys. Acta* **1780:**1236–1248; 2008.
[40] Pineyro, M. D.; Parodi-Talice, A.; Arcari, T.; Robello, C. Peroxiredoxins from Trypanosoma cruzi: virulence factors and drug targets for treatment of Chagas disease? *Gene* **408:**45–50; 2008.
[41] Rouhier, N.; Kauffmann, B.; Tete-Favier, F.; Palladino, P.; Gans, P.; Branlant, G.; Jacquot, J. P.; Boschi-Muller, S. Functional and structural aspects of poplar cytosolic and plastidial type A methionine sulfoxide reductases. *J. Biol. Chem.* **282:** 3367–3378; 2007.
[42] Lee, B. C.; Lee, Y. K.; Lee, H. J.; Stadtman, E. R.; Lee, K. H.; Chung, N. Cloning and characterization of antioxidant enzyme methionine sulfoxide-S-reductase from *Caenorhabditis elegans*. *Arch. Biochem. Biophys.* **434:**275–281; 2005.
[43] Schmidt, H.; Krauth-Siegel, R. L. Functional and physicochemical characterization of the thioredoxin system in Trypanosoma brucei. *J. Biol. Chem.* **278:**46329–46336; 2003.
[44] Holst, M.; Kozack, R. E.; Saied, F.; Subramaniam, S. Treatment of electrostatic effects in proteins: multigrid-based Newton iterative method for solution of the full nonlinear Poisson–Boltzmann equation. *Proteins* **18:**231–245; 1994.
[45] Souza, J. M.; Radi, R. Glyceraldehyde-3-phosphate dehydrogenase inactivation by peroxynitrite. *Arch. Biochem. Biophys.* **360:**187–194; 1998.
[46] Boschi-Muller, S.; Azza, S.; Sanglier-Cianferani, S.; Talfournier, F.; Van Dorsselear, A.; Branlant, G. A sulfenic acid enzyme intermediate is involved in the catalytic mechanism of peptide methionine sulfoxide reductase from Escherichia coli. *J. Biol. Chem.* **275:**35908–35913; 2000.
[47] Kelly, J. M.; Taylor, M. C.; Smith, K.; Hunter, K. J.; Fairlamb, A. H. Phenotype of recombinant Leishmania donovani and Trypanosoma cruzi which over-express trypanothione reductase: sensitivity towards agents that are thought to induce oxidative stress. *Eur. J. Biochem.* **218:**29–37; 1993.
[48] Piacenza, L.; Peluffo, G.; Alvarez, M. N.; Kelly, J. M.; Wilkinson, S. R.; Radi, R. Peroxiredoxins play a major role in protecting Trypanosoma cruzi against macrophage- and endogenously-derived peroxynitrite. *Biochem. J.* **410:** 359–368; 2008.
[49] St John, G.; Brot, N.; Ruan, J.; Erdjument-Bromage, H.; Tempst, P.; Weissbach, H.; Nathan, C. Peptide methionine sulfoxide reductase from Escherichia coli and Mycobacterium tuberculosis protects bacteria against oxidative damage from reactive nitrogen intermediates. *Proc. Natl Acad. Sci. USA* **98:**9901–9906; 2001.
[50] Cabreiro, F.; Picot, C. R.; Perichon, M.; Friguet, B.; Petropoulos, I. Overexpression of methionine sulfoxide reductases A and B2 protects MOLT-4 cells against zinc-induced oxidative stress. *Antioxid. Redox Signaling* **11:**215–225; 2009.
[51] Holland, H. L.; Gu, J. X.; Orallo, F.; Camina, M.; Fabeiro, P.; Willetts, A. J. Enantioselective synthesis and pharmacological evaluation of a new type of verapamil analog with hypotensive and calcium antagonist activities. *Pharm Res* **16:**281–287; 1999.